

1 **Title: Influence of socio-ecological factors on COVID-19 risk: a cross-sectional study based**
2 **on 178 countries/regions worldwide**

3 Dai Su^{1,2,3}, Yingchun Chen^{1,2}, Kevin He³, Tao Zhang⁴, Min Tan^{1,2}, Yunfan Zhang^{1,2}, Xingyu
4 Zhang⁵

5 1 Department of Health Management, School of Medicine and Health Management, Tongji
6 Medical College, Huazhong University of Science and Technology, Wuhan, China

7 2 Research Center for Rural Health Services, Hubei Province Key Research Institute of
8 Humanities and Social Sciences, Wuhan, China

9 3 Department of Biostatistics, University of Michigan School of Public Health, Ann
10 Arbor, United States

11 4 Department of Epidemiology and Health Statistics, West China School of Public Health and
12 West China fourth Hospital, Sichuan University, Sichuan, China

13 5 Department of Systems, Populations, and Leadership, University of Michigan School of
14 Nursing, Ann Arbor, United States

15

16 Corresponding to:

17 Xingyu Zhang (zhangxyu@umich.edu)

18 Department of Systems, Populations, and Leadership,

19 University of Michigan School of Nursing

20 Ann Arbor, Michigan

21

22 Yingchun Chen (chenyingchunhust@163.com)

23 Department of Health Management,

24 School of Medicine and Health Management,
25 Tongji Medical College, Huazhong University of Science and Technology,
26 Wuhan, China

27

28 **Word count (abstract): 140; Word count (text): 5304**

29

30

31

32

33

34

35

36

37

38

39

40

41

42

43 **Abstract**

44 The initial outbreak of COVID-19 caused by SARS-CoV-2 in China in 2019 has been severely
45 tested in other countries worldwide. We established the Potential Risk Assessment Framework
46 for COVID-19. We used spatial econometrics method to assess the global and local correlation
47 of COVID-19 risk indicators. To estimate the adjusted IRR, we modelled negative binomial
48 regression analysis with spatial information and socio-ecological factors. We found that 37, 29
49 and 39 countries/regions were strongly opposite from the IR, CMR and DCI index "spatial
50 autocorrelation hypothesis", respectively. The IR, CMR and DCI were significantly associated
51 with some socio-economic factors. We also found that climatic factors (temperature, relative
52 humidity, precipitation and wind speed) did not significantly reduce COVID-19 risk. To fight
53 against COVID-19 more effectively, countries/regions should pay more attention to controlling
54 population flow, improving diagnosis and treatment capacity, and improving public welfare
55 policies.

56 **Keywords:** socio-ecological factors; COVID-19 risk; cross-sectional study; 178
57 countries/regions worldwide

58

59

60

61

62

63

64 **1. Introduction**

65 The novel coronavirus disease (COVID-19) that has spread to more than one hundred countries
66 and killed hundreds of thousands of people has officially been categorized as a pandemic by the
67 World Health Organization. The initial outbreak of COVID-19 caused by SARS-CoV-2 in China
68 in 2019 has been severely tested in other countries worldwide. As of April 6, 2020, COVID-19
69 had infected 1,345,048 patients in 184 countries/regions and caused 74,565 deaths, as countries
70 worldwide responded to a human-to-human respiratory disease pandemic caused by COVID-19.
71 Emerging infectious diseases (EIDs), such as SARS and COVID-19, pose a vast economic and
72 public health burden worldwide [1,2].

73 COVID-19 not only seriously endangers people's life safety and health but also greatly affects
74 economic globalization. To address the challenges posed by COVID-19, the links among the
75 transmission of COVID-19, socio-economic factors and climatic factors must be understood to
76 suggest better strategies for predicting, preventing, coping with and mitigating the associated
77 challenges. Simultaneously, given that the climate and socio-economic context are unlikely to
78 change in the short term, it is easier to intervene accordingly [3]. The spread of many EIDs has
79 been reported to be influenced by socio-ecological factors, including socio-economic and climate
80 factors [1,2,4–7]. Previous studies have found that climatic conditions limit the geographical and
81 seasonal distribution of EIDs, and weather affects the timing and intensity of outbreaks [8–12].
82 In addition, whereas climate patterns may control the potential global distribution of EIDs, the
83 actual size and spatial scope of a region may be controlled by several non-climatic factors
84 associated with transmission, including epidemiological, socio-economic and demographic
85 factors [13–18]. However, research on the climatic and socio-economic drivers of COVID-19
86 transmission remains lacking, especially regarding the effects of socio-economic factors and the

87 total effects of socio-ecological factors. Ignoring important non-climatic factors or other
88 confounding factors (such as urban development, economic growth, poverty, health,
89 infrastructure, science and technology, social security and labor) would overestimate the effects
90 of climate change. Therefore, studying the influence of socio-ecological factors on the
91 transmission risk of EIDs is highly important.

92 For most EIDs, three elements are essential: an agent (or pathogen), a host (or vector) and the
93 environment of transmission [19]. Appropriate climatic and weather conditions are necessary for
94 the survival, reproduction, distribution and transmission of disease pathogens, vectors and hosts.
95 Therefore, changes in climate or weather conditions may affect EIDs by affecting pathogens,
96 vectors, hosts and their living environments [19–21]. Although many climate variables may
97 influence the transmission of EIDs, some studies have shown that changes in the four main
98 variables have the greatest effects on infected diseases with strong environmental components
99 (temperature, precipitation, relative humidity (RH) and wind) [22–26]. In recent studies,
100 although the severity of some cases of COVID-19 has mimicked that of SARS-CoV cases [27–
101 30], the reproductive number (average $R_0=3.28$) of COVID-19 is higher than that of SARS-CoV;
102 therefore, considering the climate and environment may improve understanding of the
103 pathogen’s vectorial capacity and basic reproduction number, and the risk of transmission of
104 COVID-19 [31,32].

105 In recent decades, many rapid and pronounced changes in human social ecology have altered the
106 likelihood of the emergence and spread of infectious diseases [33–35]. These changes include
107 increases in population size and density; urbanization; persistent poverty (especially in the
108 expansion of urban slums); the number and movement of political, economic and environmental
109 refugees; differences in infrastructure and science and technology; and poor health awareness

110 [36]. The socio-economic environment contributes significantly to the health of individuals as
111 well as communities [37] and is the root cause of health and health equity. These socio-economic
112 drivers have contributed to the shifting global ecology of vector transmission that enabled
113 COVID-19 to emerge worldwide, by dangerously uniting the human hosts, vectors and pathogen.
114 Socioeconomic changes interact with environmental changes in promoting EID spread and
115 increase the harm of EIDs to humans.

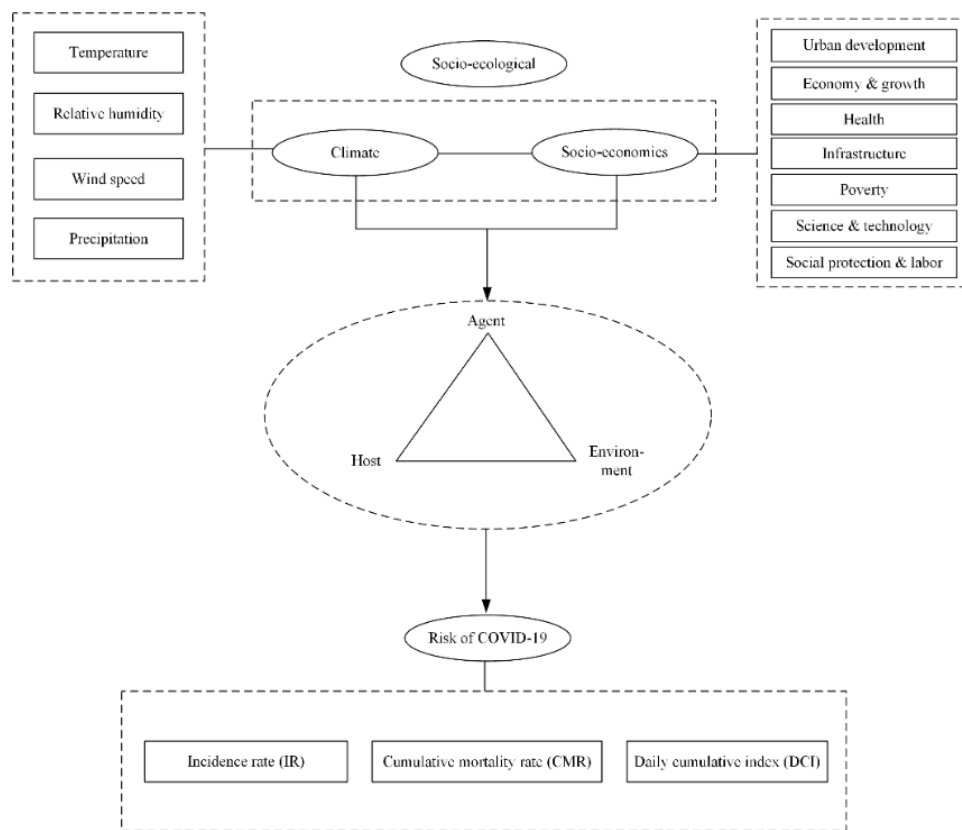
116 The purpose of this study was to describe the spatial distribution of the COVID-19 pandemic
117 worldwide, and assess the effects of different socio-ecological factors, including climate and
118 socio-economic factors, on COVID-19 risk in 178 countries/regions worldwide, including
119 incidence rate (IR), cumulative mortality rate (CMR) and daily cumulative index (DCI). In
120 addition, this study analyzed intervention policies in different countries and regions to establish
121 early warning and decision support systems and provide guidance for COVID-19 management in
122 different countries/regions.

123

124 **2. Methods**

125 **2.1. Concept model**

126 According to previous research [38–41], we established the Potential Risk Assessment
127 Framework for COVID-19 (Figure 1). The influence of global socio-ecological factors (climate
128 and socio-economic factors) on the risk of COVID-19 can be tested by its influence on the
129 following three disease components: agent (or pathogen), host (or vector) and the environment of
130 transmission. A combination of natural and human influences led to the COVID-19 pandemic.
131 We used three main variables to assess the potential risk of COVID-19: IR, CMR and DCI.



132

133 **Figure 1. Climate, socio-economic conditions and COVID-19 transmission**

134 **2.2 Definitions of different cases for COVID-19**

135 A confirmed case of COVID-19 infection was defined by laboratory confirmation of the virus
136 causing COVID-19 infection, regardless of clinical signs and symptoms [42–44]. However, some
137 reported case numbers from China have included people with symptoms of COVID-19 without
138 laboratory confirmation. The definitions of COVID-19 related deaths differ across countries. In
139 Italy, any death of a person with positive reverse transcriptase–polymerase chain reaction (RT-
140 PCR) testing for SARS-CoV-2 is considered COVID-19 related.

141 **2.3 Data collection**

142 **2.3.1 Outcome variables**

143 A dashboard published and hosted by researchers at the Center for Systems Science and
 144 Engineering, Johns Hopkins University (JHU-CSSE) [45] shows the numbers and locations of
 145 confirmed COVID-19 cases, deaths and recoveries in all affected countries. All collected data on
 146 COVID-19 from the Johns Hopkins University are made freely available by the researchers
 147 through a GitHub repository. All manual updates (for countries and regions outside mainland
 148 China) are coordinated by a team at Johns Hopkins University. We extracted the global time
 149 series data of confirmed and recovered cases and deaths due to COVID-19 from the JHU-CSSE
 150 GitHub repository. The data were recorded from January 22, 2020 and were updated once daily
 151 around 23:59 (UTC). We selected the cross-sectional data from April 6, 2020. On the basis of the
 152 availability of the data, we extracted 178 countries from the database (excluding
 153 countries/regions without COVID-19 cases and some unmatched countries/regions, such as
 154 Taiwan, China). The first-level geographical unit of the dataset is the country/region, and the
 155 second-level geographical unit is the province/state. We uniformly selected first-level
 156 geographical units (countries/regions). In addition, we further classified the countries/regions in
 157 the data set according to UN geographical divisions and divided the countries with epidemic
 158 COVID-19 into 20 regions. As previously mentioned, for outcome variables, we selected IR,
 159 CMR and DCI as indicators to measure COVID-19 risk. The specific calculation process is
 160 shown in Table 1.

Table 1 The calculation process of outcome variables for COVID-19

Outcome variables	Calculation process
Incidence rate (IR)	$IR = \frac{\text{Number of new cases of COVID-19 in a given time period}}{\text{Total population at risk during the follow-up period}} \times 1,000,000$
Cumulative mortality rate (CMR)	$CMR = \frac{\text{number of COVID-19 deaths in a given time period}}{\text{total population during a given time period}} \times 1,000,000$

Daily cumulative index (DCI)	$DCI = \frac{\text{cumulative COVID-19 confirmed cases}}{\text{number of days between the first reported case until now}}$
---------------------------------	--

161

162 IR was used to describe the distribution of COVID-19, explore the etiological factors, propose an
163 etiological hypothesis, and evaluate the efficacy of detection and prevention measures. CMR
164 reflects the total deaths due to COVID-19 and is an indicator of the risk of death from COVID-
165 19. DCI mainly describes the growth rate of COVID-19 in different countries/regions and is a
166 measure of the risk of disease transmission. The World Health Organization, on March 11, 2020,
167 declared the COVID-19 outbreak a global pandemic, thus indicating that COVID-19 had broadly
168 spread worldwide. Therefore, when we considered IR, CMR and DCI in different
169 countries/regions, these measures reflected not only the rapid growth in the number of people
170 infected with COVID-19 but also the detection level in the entire country/region, which was used
171 to identify more people infected with COVID-19.

172 **2.3.2 Climate data**

173 We obtained daily meteorological observation values from the Global Surface Summary of the
174 Day (GSOD) via The Integrated Surface Hourly (ISH) dataset. The ISH dataset includes global
175 data obtained from the USAF Climatology Center, which is located in the Federal Climate
176 Complex with NCDC. GSOD comprises 12 daily averages computed from global hourly station
177 data. Except in United States stations, 24-hour periods are based on UTC times. The latest daily
178 summary data are normally available 1–2 days after the date-time of the observations used in the
179 daily summaries. More than 9,000 stations' data worldwide are typically available. Daily weather
180 elements include mean values of temperature, dew point temperature, sea level pressure, station
181 pressure, visibility, wind speed, maximum and minimum temperature, maximum sustained wind

182 speed and maximum gust, precipitation amount, snow depth and weather indicators. However,
183 we chose the climate data from April 6, 2020 and selected four variables from the GSOD dataset
184 that significantly affected COVID-19 risk: (1) mean temperature (.1 Fahrenheit); (2) mean dew
185 point (.1 Fahrenheit); (3) mean wind speed (.1 knots); and (4) precipitation amount (.01 inches).
186 The reason for extracting the average dew point variable was to calculate the RH value by using
187 this variable and the temperature variable. The temperature and dew point in Celsius were used
188 to calculate the RH according to the temperature and dew point at each time point [46]:

$$189 \quad C = \frac{F - 32}{1.8}$$

$$190 \quad RH = e^{\frac{17.625D}{243.04+D} - \frac{17.625T}{243.04+T}}$$

191 where C is the temperature in Celsius, F is the temperature in Fahrenheit, D is the mean dew
192 point for the day in Celsius, T is the mean temperature for the day in Celsius, and e is the base
193 of the natural log.

194 **2.3.3 Socio-economic data**

195 Indicators of socio-economic factors affecting the spread of COVID-19 were derived from the
196 World Development Indicators dataset, the primary World Bank collection of development
197 indicators, which compiles relevant, high-quality and internationally comparable statistics about
198 global development and the fight against poverty. The database contains 1,600 time series
199 indicators for 217 economies and more than 40 country groups, and data for many indicators
200 cover a period of more than 50 years. As shown in Table 2, we selected 32 indicators affecting
201 COVID-19 risk in seven dimensions in 178 countries/regions. The index value for 2019 was

202 taken as the priority for each indicator. If the index was missing in 2019, the index value of the
 203 most recent year was selected as a substitute.

Table 2. Socioeconomic indicators influencing the spread of COVID-19

Dimensions	Indicators	No.	
Urban Development	Urban population (% of total population)	(1)	
	Urban population growth (annual %)	(2)	
	Population density (people per sq. km of land area)	(3)	
Economy & Growth	GDP per capita (current US\$)	(4)	
Health	People using at least basic sanitation services (% of population)	(5)	
	Current health expenditure (% of GDP)	(6)	
	Current health expenditure per capita (current US\$)	(7)	
	Death rate, crude (per 1,000 people)	(8)	
	Domestic private health expenditure (% of current health expenditure)	(9)	
	Domestic private health expenditure per capita (current US\$)	(10)	
	Hospital beds (per 1,000 people)	(11)	
	Life expectancy at birth, total (years)	(12)	
	Maternal mortality ratio (national estimate, per 100,000 live births)	(13)	
	Mortality rate, infant (per 1,000 live births)	(14)	
	Net migration	(15)	
	Nurses and midwives (per 1,000 people)	(16)	
	People with basic handwashing facilities including soap and water (% of population)	(17)	
	Physicians (per 1,000 people)	(18)	
	Population aged 65 and above (% of total population)	(19)	
	Population growth (annual %)	(20)	
	Proportion of population spending more than 10% of household consumption or income on out-of-pocket health care expenses (%)	(21)	
	Proportion of population spending more than 25% of household consumption or income on out-of-pocket health care expenses (%)	(22)	
	Infrastructure	Railways, passengers carried (million passenger-km)	(23)
	Poverty	Poverty headcount ratio at national poverty lines (% of population)	(24)
	Science & Technology	Researchers in R&D (per million people)	(25)
		Technicians in R&D (per million people)	(26)

Social Protection & Labor	Coverage of social insurance programs (% of population)	(27)
	Unemployment, total (% of total labor force) (national estimate)	(28)

204

205 2.4 Statistical analysis

206 2.4.1. Spatial econometrics method

207 First, we used Moran's I to measure the global correlation of COVID-19 risk indicators [47].

208 Global Moran's I is a measure of global spatial autocorrelation, and the value of Moran's I

209 usually ranges from -1 to $+1$. Values significantly below $-1/(N-1)$ indicate negative spatial

210 autocorrelation, and values significantly above $-1/(N-1)$ indicate positive spatial autocorrelation.

211 If significant global spatial autocorrelation was found, we then used local indicators of spatial

212 autocorrelation (LISA) to evaluate the locations of COVID-19 clusters. The meaning of local

213 Moran's I_i is similar to that of global Moran's I. A positive I_i indicates that the high (or low)

214 value of region i is surrounded by the surrounding high (or low) value; A negative I_i indicates

215 that the high (or low) value of region i is surrounded by the surrounding low (or high) value. The

216 general models are described in Eq. 1–2.

$$217 \text{ Moran's } I = \frac{n \sum_{i=1}^n \sum_{j=1}^n w_{ij} (x_i - \bar{x})(x_j - \bar{x})}{n \sum_{i=1}^n \sum_{j=1}^n w_{ij} \sum_{i=1}^n (x_i - \bar{x})^2} \quad (1)$$

$$218 \text{ Local Moran's } I = \frac{n(x_i - \bar{x}) \sum_j w_{ij} (x_j - \bar{x})}{\sum_i (x_i - \bar{x})^2} \quad (2)$$

219 where n is the number of spatial units indexed by i and j , x is the variable of social ecology
220 factors, \bar{x} is the mean of x , and w_{ij} is a matrix of spatial weights with zeroes on a diagonal (i.e.,
221 $w_{ii}=0$).

222 Second, to better approximate the real infectious disease spatial spread process, we fit a one-
223 order spatial autoregressive regression model comprising spatial lags. Because we believed that
224 COVID-19 risk transmission in a certain country/region would be different for neighboring
225 countries/regions, we sought to reflect this difference in the model. A one-order spatial
226 autoregressive process takes the form (Eq. 3) [48]:

$$227 \quad Y = \delta WY + \varepsilon \quad (3)$$

228 where δ is the spatial autoregressive coefficient, W is the i, j -th element of the exogenous,
229 non-negative $N \times N$ spatial weight matrix with zero diagonal elements that describes the
230 arrangement of the spatial units in the countries/regions, and ε is i.i.d. innovations with zero
231 mean and finite variance σ^2 . For simplicity, in this paper, we assumed that the spatial weight
232 matrix W was non-standardized and also used a queen spatial weight matrix.

233 2.4.2. Processing of missing values

234 Before negative binominal regression, the k-nearest neighbors (k-NN) approach was used to
235 impute missing data for some socio-ecological variables. For a given patient with missing values,
236 the k-NN method identifies the k-nearest countries/regions on the basis of Euclidean distance.
237 Using these countries/regions, we then replaced missing values by using a majority vote for
238 discrete variables and weighted means for continuous features. One advantage of using this

239 method is that missing values in all features are imputed simultaneously without the need to treat
240 features individually.

241 2.4.3. Negative binomial regression

242 First, we established the correlation matrix of socio-economic factors to check for
243 multicollinearity. If there was a strong correlation (> 0.8) among socio-economic factors, then
244 we removed the factor with strong correlation with other variables. Then, the incidence rate ratio
245 (IRR) of each socio-ecological factor was calculated with single factor negative binomial
246 regression analysis, that is, the effect of each socio-ecological factor on COVID-19 risk by
247 changing the average COVID-19 risk value by a specific unit quantity. The spatial autoregressive
248 models comprising spatial lags, which were a weighted average of observations on the diseases
249 over neighboring units, were input into the model to adjust for spatial variation in COVID-19
250 risk. Modeled values of climate factors were centered on the mean values for each station in
251 every country/region [49]. The factors with $P < 0.05$ were included in the multi-factor negative
252 binomial regression analysis with spatial information to calculate the adjusted IRR (aIRR). The
253 general model is described in Eq. 4.

$$254 \quad y_i = \alpha + \delta WY + \beta_1 T_i + \beta_2 H_i + \beta_3 M_i + \beta_4 P_i + \sum S_n + \varepsilon_i \quad (4)$$

255 where y_i denotes the daily counts of COVID-19 risk indicators in county/region i ; WY
256 represents spatial lags, and W is the spatial weight; S_n represents socio-economic factors (all
257 variables are in Table 2); T_i is the mean temperature in county/region i ; H_i is the RH in
258 county/region i ; M_i is the wind speed in county/region i ; P_i is the precipitation amount in
259 county/region i ; and ε_i is a random intercept.

260 Sensitivity analyses with maximum and minimum temperatures instead of average temperatures
261 were also conducted with the same procedures, in which we used the same non-informative
262 priors for the minimum and maximum temperatures [49, 50]. All statistical analyses were
263 performed in Stata statistical software Version 15, and p-values were two-tailed, with statistical
264 significance set at .05. ArcMap 10.7 and Geoda software were used to process basic geographic
265 information. Data visualization mainly used RStudio software Version 1.2.5033.

266 **2.4 Patient and public involvement**

267 This research was done without patient involvement. Patients were not invited to comment on
268 the study design and were not consulted to develop patient relevant outcomes or interpret the
269 results. Patients were not invited to contribute to the writing or editing of this document for
270 readability or accuracy.

271

272 **3. Results**

273 **3.1 Characteristics of 178 countries/regions with reported cases of COVID-19**

274 As of April 6, 2020, a total of 178 countries/regions worldwide had reported data and were
275 included in this study (Table S1). The three countries/regions with the highest IR worldwide
276 were Andorra (Southern Europe, IR=313.80), Iceland (Northern Europe, IR=215.90) and
277 Gibraltar (United Kingdom) (Southern Europe, IR=178.52). The three countries/regions with the
278 highest CMR worldwide were San Marino (Southern Europe, CMR=947.17), Spain (Southern
279 Europe, IR=285.53) and Italy (Southern Europe, IR=273.42). The three countries/regions with
280 the highest DCI worldwide were the United States (North America, DCI=4823.87), Spain
281 (Southern Europe, DCI=2070.83) and Italy (Southern Europe, DCI=1978.31).

Table 3 Characteristics of UN geographical divisions with reported cases of COVID-19 as of 6 April 2020

UN* geographical divisions	No. of Countries/regions	IR†	CMR‡	DCI§	Total population	Total days since first reported case
Africa						
Eastern Africa	17	0.18	0.04	2.85	451173502	325
Middle Africa	8	0.12	0.21	4.96	168910830	189
Northern Africa	5	1.92	1.85	25.03	194924933	179
Southern Africa	3	0.50	0.21	26.28	62482003	65
Western Africa	13	0.35	0.16	4.93	343169384	299
Asia						
Central Asia	3	4.55	0.21	19.63	57547699	68
East Asia	4	0.40	2.29	355.28	1574064564	273
Southeast Asia	9	1.47	0.78	26.75	600191804	525
Southern Asia	9	2.18	2.09	159.97	1896189013	436
Western Asia	14	11.32	1.67	36.21	138585525	586
Europe						
Eastern Europe	10	6.91	1.85	64.50	292450026	379
Northern Europe	12	51.86	60.72	153.93	104678611	528
Southern Europe	14	64.24	204.80	535.26	148744007	541
Western Asia	1	38.24	7.88	1119.15	82319724	27
Western Europe	9	57.69	77.55	628.85	196616151	442
North America						
Caribbean	16	3.35	2.99	7.62	38841019	338
Central America	8	2.86	1.03	24.87	175471759	203
North America	4	83.30	30.53	2027.60	364346283	189
Oceania						

Australia and New Zealand	2	5.92	1.37	62.19	29877869	111
Melanesia	5	0.49	0.00	1.92	22465856	106
South America	12	4.74	2.39	74.46	423398995	367

*UN, United Nations.

†IR, incidence rate (per 10 million people).

‡CMR, cumulative mortality rate (per 10 million people).

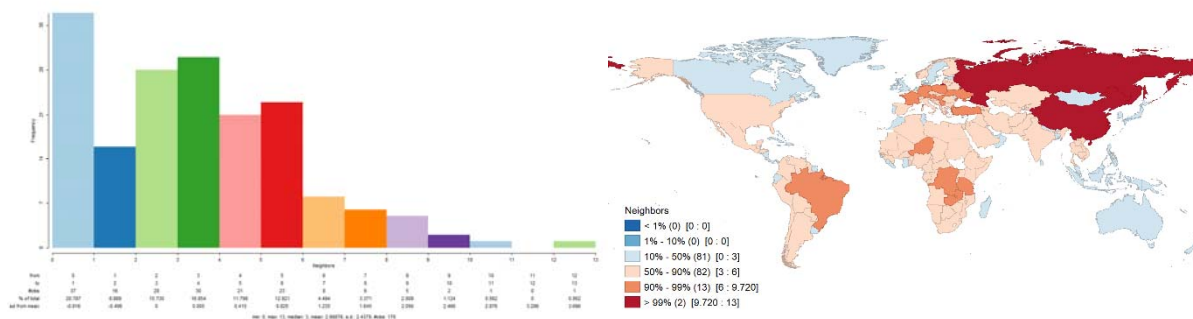
§DCI, daily cumulative index (%)

282

283 **3.2 Spatial clustering evaluation for COVID-19**

284 3.2.1 Test results for global spatial correlation

285 The number and distribution of first-order neighbors in different countries/regions are shown in
 286 Figure 2. The number of neighboring countries/regions was mainly concentrated in 0–6,
 287 accounting for 87.08% of the total number of neighboring countries. Among them, China and
 288 Russia had the largest number of neighboring countries/regions.



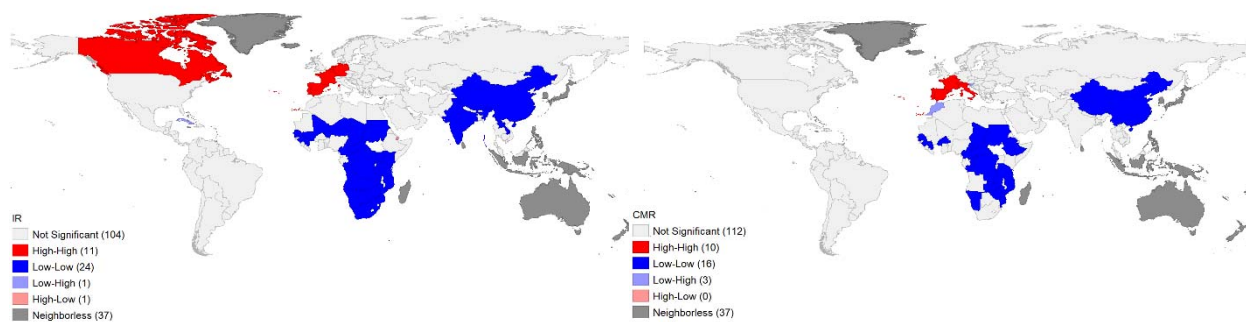
289
 290 **Figure 2. Number and distribution of first-order neighbors in different countries/regions**

291 Table S2 shows the global spatial Moran's I indexes of the IR, CMR and DCI of 178
 292 countries/regions worldwide according to the one-order spatial contiguity matrix. The Moran's I
 293 indexes of IR, CMR and DCI were all positive, and all index values were significant at the level
 294 of 1%, thus indicating that the IR, CMR and DCI of 178 countries/regions worldwide had strong
 295 spatial aggregation effects. Meanwhile, the Moran's I index of different indicators showed
 296 significant differences, thus indicating to some extent that IR, CMR and DCI have different
 297 aggregation effects in different countries/regions.

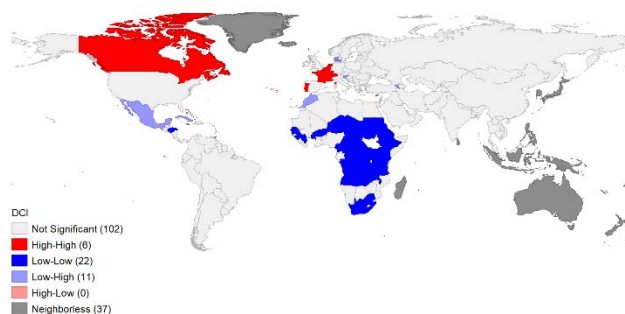
298 3.2.2 Test results for local spatial correlation

299 Figure 3 shows the world map with local Moran's I for IR, CMR and DCI indicators in some
300 countries/regions at a significance level of 10%. A total of 37 countries/regions were strongly
301 opposite from the IR index "spatial autocorrelation hypothesis," including 11 countries/regions
302 with high–high patterns, mainly concentrated in Western Europe, southern Europe and Canada;
303 24 countries/regions with low–low patterns, mainly concentrated in parts of Africa, parts of Asia
304 (China, India, Laos); Cuba with a low–high pattern; and Djibouti with a high–low pattern.
305 Simultaneously, 29 countries/regions were strongly opposite from the CMR index "spatial
306 autocorrelation hypothesis," which was suitable for 10 countries with high–high patterns, mainly
307 in Western Europe and southern Europe (e.g., France, Italy and Spain); 16 countries/regions with
308 low–low patterns, mainly concentrated in parts of Africa and China; and three countries with
309 low–high patterns, including Morocco and Slovenia. In addition, 39 countries/regions strongly
310 did not support the hypothesis of "no spatial autocorrelation" of the DCI index, among which six
311 countries/regions had high–high patterns (Canada, France, Portugal, Belgium, the Netherlands,
312 and Switzerland), and 22 countries/regions had low–low patterns, mainly in parts of Africa and
313 Honduras. Eleven countries were in the low–high pattern category, including Mexico, Cuba,
314 Morocco, Denmark and Luxembourg, etc. The above results are consistent with the global spatial
315 autocorrelation test results, thus indicating that IR, CMR and DCI indicators in some
316 countries/regions may be affected by the COVID-19 epidemic in neighboring countries/regions
317 and may show clear geographical characteristics.

318



319

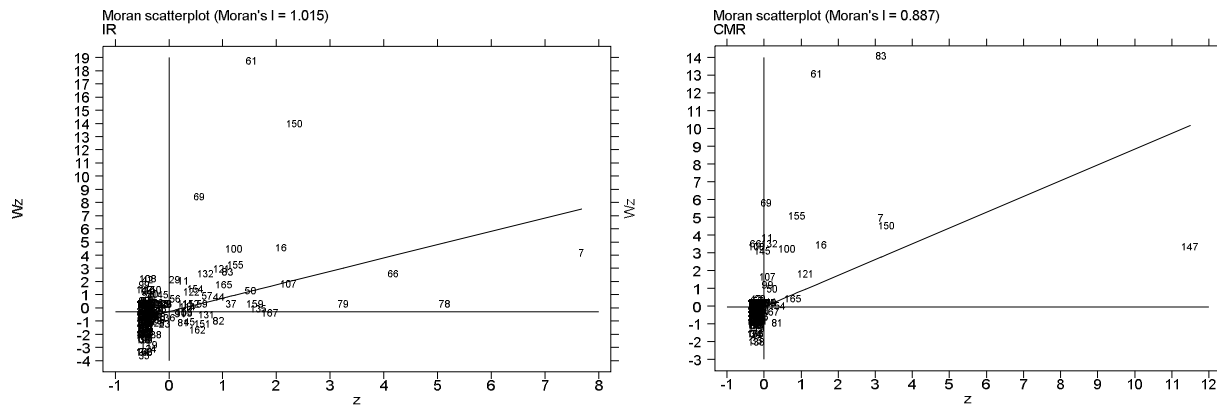


320 **Figure 3. The world map of local Moran's I of the IR, CMR and DCI indexes for COVID-**
321 **19 in some countries/regions at the 10% significance level**

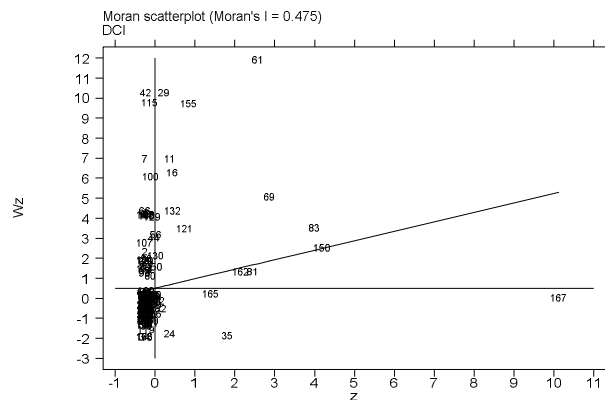
322 To directly reflect the local spatial characteristics of IR, CMR and DCI, LISA scatter diagrams
323 of the three indexes are shown in Figure 4. Most of the three indicators fell into the third
324 quadrant (low–low), but the countries/regions whose IR and DCI index fell into the first quadrant
325 (high–high) and the second quadrant (low–high) had indicator values exceeding the CMR. Thus,
326 among the 178 countries/regions worldwide, the countries/regions with low IR, CMR and DCI
327 indicators showed a spatial agglomeration effect, as did the countries/regions with high IR, CMR
328 and DCI indicators. In addition, some neighboring countries/regions showed some differences in
329 IR, CMR and DCI (high–low and low–high).

330

331



332



333 **Figure 4. LISA scatter diagram of IR, CMR and DCI indexes for COVID-19 in 178**
334 **countries/regions**

335 (z is the value of the variable, and Wz is the local Moran's Ii value of the variable.)

336

337 **3.3 Analysis of the influence of socio-ecological factors on COVID-19 risk**

338 **3.3.1 Correlation analysis of socio-economic factors**

339 To eliminate the influence of the collinearity between the socio-economic indicators on the

340 estimation effect of the model, we established a correlation matrix of the socio-economic

341 indicators (Table S3). The indexes with strong correlation (> 0.8) were screened, and one of the

342 effective indexes was reserved for model analysis. We excluded eight socio-economic indicators

343 in Table 2, numbered 7 (current health expenditure per capita), 12 (total life expectancy at birth),
344 13 (maternal mortality ratio), 14 (infant mortality rate), 17 (access to basic handwashing
345 facilities including soap and water), 20 (population growth), 21 (proportion of the population
346 spending more than 10% of household consumption or income on out-of-pocket health care
347 expenditure) and 26 (technicians in R&D), and we retained 20 socio-economic indicators.

348 3.3.2 Negative binomial regression analysis of socio-ecological factors on COVID-19 risk

349 We analyzed the effects of socio-ecological factors on COVID-19 risk in 178 countries. The
350 results of single-factor and multi-factor negative binomial regression analysis are shown in Table
351 4.

352 The IR was significantly positively associated with GDP per capita (aIRR=1.029, 95%CI: 1.013–
353 1.045), use of at least basic sanitation services (aIRR=1.022, 95%CI: 1.005–1.039) and coverage
354 of social insurance programs (aIRR=1.047, 95%CI: 1.009–1.086), and was significantly
355 negatively associated with the proportion of the population spending more than 25% of
356 household consumption or income on out-of-pocket health care expenses (aIRR=0.846, 95%CI:
357 0.750–0.955) and the poverty headcount ratio at national poverty lines (aIRR=0.970, 95%CI:
358 0.948–0.993).

359 The CMR was significantly positively associated with urban populations (aIRR=1.027, 95%CI:
360 1.010–1.044), GDP per capita (aIRR=1.031, 95%CI: 1.021–1.041) and current health
361 expenditure (aIRR=1.211, 95%CI: 1.040–1.410), and was significantly negatively associated
362 with the number of hospital beds (aIRR=0.799, 95%CI: 0.696–0.916), number of nurses and
363 midwives (aIRR=0.837, 95%CI: 0.749–0.936) and poverty headcount ratio at the national
364 poverty lines (aIRR=0.960, 95%CI: 0.940–0.982).

365 The DCI was significantly positively associated with urban populations (aIRR=1.021, 95%CI:
366 1.009–1.034), population density (aIRR=1.000, 95%CI: 1.000–1.000) and researchers in R&D
367 (aIRR=1.000, 95%CI: 1.000–1.001), and was significantly negatively associated with the
368 number of hospital beds (aIRR=0.731, 95%CI: 0.641–0.833), number of nurses and midwives
369 (aIRR=0.904, 95%CI: 0.820–0.997) and poverty headcount ratio at the national poverty lines
370 (aIRR=0.963, 95%CI: 0.945–0.982).

371 The results of the sensitivity analysis are reported in Table S4 and Table S5: we used the
372 maximum and minimum temperatures instead of the average temperature, and then incorporated
373 the two climate factors into the single-factor and multi-factor negative binomial regression. The
374 results showed that the significance of different socio-ecological factors was essentially
375 consistent. We found that only the variable of poverty headcount ratio at the national poverty
376 lines (percentage of population) became significant after sensitivity analysis on IR, thus
377 indicating that the analysis results were relatively reliable.

Table 4. The results of single-factor and multi-factor negative binomial regression analysis for COVID-19 in 178 countries/regions

Indicators	Incidence rate (IR)								Cumulative mortality rate (CMR)								Daily cumulative index (DCI)							
	IRR*	95%CI† (Lower)	95%CI (Upper)	p-value	aIRR‡	95%CI (Lower)	95%CI (Upper)	p-value	IRR	95%CI (Lower)	95%CI (Upper)	p-value	aIRR	95%CI (Lower)	95%CI (Upper)	p-value	IRR	95%CI (Lower)	95%CI (Upper)	p-value	aIRR	95%CI (Lower)	95%CI (Upper)	p-value
Urban Development																								
Urban population (% of total population)	1.048	0.992	1.106	0.096					1.055	1.027	1.083	<0.001	1.027	1.010	1.044	0.001	1.073	1.055	1.091	<0.001	1.022	1.010	1.034	<0.001
Urban population growth (annual %)	1.053	1.039	1.066	<0.001	0.866	0.670	1.120	0.273	0.287	0.203	0.405	<0.001	0.751	0.507	1.112	0.153	0.407	0.312	0.530	<0.001	0.993	0.734	1.343	0.963
Population density (people per sq. km of land area)	1.000	1.000	1.000	0.179					1.000	1.000	1.000	0.633					1.000	1.000	1.000	<0.001	1.000	1.000	1.000	0.020
Economy & Growth																								
GDP per capita (current 1,000 US\$)	1.054	1.038	1.071	<0.001	1.029	1.013	1.045	<0.001	1.086	1.056	1.117	<0.001	1.031	1.021	1.041	<0.001	1.045	1.019	1.072	0.001	0.998	0.987	1.009	0.696
Health																								
People using at least basic sanitation services (% of population)	1.063	1.048	1.078	<0.001	1.022	1.005	1.039	0.010	1.088	1.065	1.111	<0.001	1.001	0.985	1.016	0.897	1.056	1.045	1.066	<0.001	1.011	0.998	1.025	0.102
Current health expenditure (% of GDP)	1.186	1.045	1.345	0.008	1.088	0.956	1.238	0.203	1.501	1.245	1.809	<0.001	1.211	1.040	1.416	0.013	1.416	1.216	1.648	<0.001	1.080	0.968	1.206	0.169
Death rate, crude (per 1,000 people)	0.954	0.862	1.057	0.371					1.097	0.857	1.403	0.462					1.187	0.978	1.439	0.082				
Domestic private health expenditure (% of current health expenditure)	0.955	0.933	0.978	<0.001	0.988	0.972	1.004	0.135	0.937	0.906	0.969	<0.001	0.986	0.970	1.000	0.102	0.951	0.933	0.970	<0.001	1.010	0.994	1.027	0.207
Domestic private health expenditure per capita (current US\$)	1.003	1.002	1.003	<0.001	1.001	1.000	1.001	0.119	1.005	1.003	1.008	<0.001	1.001	1.000	1.000	0.104	1.003	1.001	1.004	<0.001	1.000	1.000	1.001	0.438
Hospital beds (per 1,000 people)	1.246	1.034	1.502	0.021	0.906	0.790	1.039	0.156	1.798	1.067	3.030	0.028	0.799	0.696	0.911	0.001	1.302	1.022	1.659	0.033	0.731	0.641	0.833	<0.001
Net migration	1.000	1.000	1.000	<0.001	1.000	1.000	1.000	0.954	1.000	1.000	1.000	0.001	1.000	1.000	1.000	0.530	1.000	1.000	1.000	0.005	1.000	1.000	1.000	0.103
Nurses and midwives (per 1,000 people)	1.239	1.149	1.337	<0.001	0.901	0.813	1.002	0.052	1.499	1.268	1.773	<0.001	0.837	0.749	0.933	0.002	1.290	1.111	1.498	0.001	0.904	0.820	0.997	0.044
Physicians (per 1,000 people)	1.938	1.393	2.698	<0.001	1.005	0.750	1.347	0.972	3.389	2.652	4.331	<0.001	1.725	1.191	2.499	0.004	2.600	1.739	3.886	<0.001	0.951	0.758	1.192	0.661
Population ages 65 and above (% of total population)	1.111	1.054	1.171	<0.001	0.981	0.913	1.055	0.609	1.235	1.151	1.326	<0.001	1.066	0.968	1.177	0.192	1.233	1.144	1.328	<0.001	1.062	0.988	1.141	0.102
Proportion of population spending more than 25% of household consumption or income on out-of-pocket health care expenditure (%)	0.802	0.675	0.953	0.012	0.846	0.750	0.955	0.007	0.794	0.626	1.007	0.057					0.898	0.715	1.129	0.357				
Infrastructure																								
Railways, passengers carried (million passenger-km)	1.000	1.000	1.000	<0.001	1.000	1.000	1.000	0.323	1.000	1.000	1.000	0.679					1.000	1.000	1.000	0.498				
Poverty																								
Poverty headcount ratio at national poverty lines (% of population)	0.924	0.900	0.949	<0.001	0.970	0.948	0.993	0.011	0.894	0.872	0.916	<0.001	0.960	0.940	0.982	<0.001	0.908	0.889	0.926	<0.001	0.963	0.945	0.982	<0.001
Science & Technology																								
Researchers in R&D (per million people)	1.000	1.000	1.001	<0.001	1.000	1.000	1.000	0.159	1.000	1.000	1.001	0.034	1.000	1.000	1.000	0.115	1.001	1.001	1.001	<0.001	1.000	1.000	1.001	0.012
Social Protection & Labor																								
Coverage of social insurance programs (% of population)	1.060	1.041	1.079	<0.001	1.047	1.009	1.086	0.014	1.036	0.992	1.082	0.110					1.091	1.072	1.110	<0.001	1.015	0.991	1.039	0.214
Unemployment, total (% of total labor force) (national estimate)	0.902	0.828	0.982	0.018	0.956	0.909	1.004	0.072	1.002	0.861	1.166	0.984					0.986	0.866	1.122	0.828				
Climate																								
Mean temperature (Celsius)	0.934	0.897	0.972	0.001	1.039	0.992	1.088	0.105	0.975	0.887	1.071	0.592					0.834	0.800	0.869	<0.001	0.978	0.939	1.018	0.280
Relative humidity (%)	1.011	0.994	1.027	0.204					1.025	0.995	1.056	0.108					0.990	0.960	1.022	0.538				
Mean wind speed (.1 knots);	1.210	1.111	1.317	<0.001	1.040	0.957	1.130	0.358	1.155	0.951	1.403	0.146					0.958	0.836	1.097	0.533				
Precipitation amount (.01 inches).	0.082	0.016	0.003	0.003	0.477	0.126	1.808	0.276	0.019	0.001	0.377	0.009	0.425	0.123	1.471	0.177	0.204	0.005	8.409	0.402				

*IRR, incidence rate ratio.
 †CI is short for confidence interval.
 ‡aIRR, adjusted incidence rate ratio.

medRxiv preprint doi: <https://doi.org/10.1101/2020.04.23.20077545>; this version posted April 29, 2020. The copyright holder for this preprint (which was not certified by peer review) is the author/funder, who has granted medRxiv a license to display the preprint in perpetuity. It is made available under a CC-BY 4.0 International license.

380 **4. Discussion**

381 By evaluating the spatial aggregation characteristics of three indicators—IR, CMR and DCI—on
382 COVID-19 risk in 178 countries, Western Europe, Southern Europe, East Asia and some African
383 countries, we found that all showed relatively large spatial correlations, thus indicating that
384 COVID-19 broadly affects these countries/regions.

385 Because COVID-19 is highly contagious, after an outbreak occurs in a country/region, the virus
386 tends to spread rapidly in surrounding countries. Italy was the first country in Europe to have a
387 large outbreak of COVID-19, but the Italian health system adopted several control measures,
388 such as timely intervention and containment measures brought about by decentralization, flexible
389 financing mechanisms, private and public sector partnerships, and human resources mobilization,
390 so that the IR and DCI could be effectively controlled [51]. However, because some European
391 countries did not perform effective prevention and control measures, such as blockading
392 countries or cities, in early stages of the outbreak, the epidemic gradually broke out in countries
393 including France, Germany, Spain and Portugal. In North America, the development of COVID-
394 19 presents progressive characteristics (high–high and low–high mode), and Canada is also
395 significantly affect clearly the United States by the COVID–19 outbreak, but the DCI in Mexico
396 and other countries/regions in Central America remained relatively low. The United States also
397 recently closed its border with Canada and Mexico and decreased the flow of people across the
398 border. Because, blockading and quarantining provide very good protection, taking these
399 measures in countries or cities is very important to decrease the risk of COVID-19 multinational
400 spread. The potential transmission of COVID-19 in South America must not be ignored.

401 Second, both IR and CMR presented low–low patterns in China, thus indicating that China and
402 some neighboring countries (such as South Korea and Singapore) have effectively reduced the

403 risk to neighboring countries by implementing strong prevention and control measures against
404 COVID-19 transmission and have also acquired valuable experience useful to other countries in
405 fighting COVID-19 virus [52–56]. However, notably, the IR of COVID-19 in India presents a
406 low–low model, thus indicating that India is at low risk of COVID-19 transmission from
407 surrounding countries, and consequently has a low DCI. However, as the world's second most
408 populous country, India may have a high risk of COVID-19 transmission because of inadequate
409 medical conditions and detection levels. Simultaneously, China, South Korea and other countries
410 must strengthen screening of imported cases from other countries, reduce social contact among
411 travelers and prevent the possible secondary transmission of COVID-19 [52,57,58].

412 Third, most countries/regions in Africa remain in a low–low mode, but the short distance and
413 frequent contacts between Western and Southern Europe and North Africa may place North
414 Africa at high risk of COVID-19 spread; Morocco currently has a low–high mode representing
415 an early warning, and COVID-19 viruses must further be prevented from entering other parts of
416 Africa. Although African countries took measures to prevent the Ebola outbreak in 2014, Africa
417 remains one of the poorest countries worldwide, and it has a shortage of health resources to
418 quickly control the outbreak. Studies have shown that the current spread of COVID-19 in West
419 Africa urgently requires action to control the further spread of COVID-19 and improve the
420 response capacity of affected countries in West Africa [59]. Although most parts of Africa are in
421 the low–low mode, they may also face threats. Many COVID-19 cases may be undetected, thus
422 potentially explaining the current low-level indicators (IR, CMR and DCI).

423 We found that, in terms of urban development, both CMR and DCI had significant positive
424 effects on the urban population (percentage home of total population), and people per sq. km of
425 land area had significant positive effects on the DCI. Non-drug intervention measures have

426 already been implemented, and if traffic restrictions, social isolation and family measures are not
427 ensured, the increase in population density and urbanization may result in many problems, such
428 as public traffic, rural population health inequities, poor housing conditions, inadequate
429 freshwater supply, and poor sanitation and ventilation systems, thus accelerating the spread of
430 the COVID-19 virus, in agreement with previous research [60,61]. The higher the urban
431 population (percentage of total population), the faster the urbanization process of the
432 country/region; consequently, aging and young people participating in social activities become
433 more likely to aggravate the spread of the virus and increase the burden on the health system, in
434 agreement with the results of one study [62]. In addition, studies have shown that, with
435 urbanization, the risk of infection and the chances of survival after COVID-19 infection among
436 older individuals with complications is greatly increased, thus resulting in a significant increase
437 in the CMR in the country/region [63–64].

438 In terms of the economy and growth, we found that GDP per capita (current 1,000 US\$)
439 significantly improved the IR and CMR of COVID-19, possibly because the GDP per capita
440 tends to reflect a country's economic development level: with higher GDP per capita,
441 governments can invest more in screening and treatment of patients with mild and severe cases
442 of COVID-19. Consequently, with more confirmed cases and deaths, classification strategies can
443 be considered for COVID-19 in low-income groups. Especially in economically underdeveloped
444 areas such as Africa, similar symptoms can be used as a basis to implement a series of diagnostic
445 tests [65]. This method of raising clinical diagnostic standards was used in Wuhan, China.

446 In terms of health, we found that increasing the proportion of residents using at least basic
447 sanitation services can significantly improve the IR of COVID-19. For example, improving basic
448 sanitation services and increasing contact between primary health workers and potential and

449 diagnosed COVID-19 patients is very important. In particular, the government of Wuhan, China
450 implemented nucleic acid testing on each resident via hospitals and primary health workers, thus
451 enabling COVID-19 detection in a larger proportion and facilitating rapid control of COVID-19
452 risk transmission. Second, the numbers of hospital beds (per 1,000 people), nurses and midwives
453 (per 1,000 people) negatively affects the IR and CMR of COVID-19, thus suggesting that
454 COVID-19 risk should be controlled, and the number of hospital beds and nurses should be
455 increased in a short period of time. The increase in the numbers of hospital beds and nurses can
456 help achieve standardized management of patients and allow more medical resources to be
457 concentrated on the treatment of severe cases. Some research has shown that some countries,
458 such as Italy, China and the United States, have established Fangcang shelter hospitals or field
459 hospitals and increased the numbers of regular hospital beds, intensive care beds and medical
460 workers (by transferring resources from other regions and the military), reopened closed
461 hospitals, and considered use of medical volunteers in the treatment of mild and severe COVID-
462 19 cases; these measures are effective ways to reduce the IR and CMR [66, 67]. Third, among
463 people infected with COVID-19, the proportion of the population spending more than 25% of
464 household consumption or income on out-of-pocket health care expenses negatively influences
465 the IR, whereas coverage with social insurance plans positively influences the IR. Higher income,
466 enhanced health insurance coverage and decreased burden of medical treatment significantly
467 increase the IR, thus suggesting that governments and health insurance providers should
468 cooperate in the prevention and control of COVID-19. In addition to financial subsidies, the
469 government should also reduce or grant exemptions for patient co-payments, to increase the
470 possibility of COVID-19 patients receiving testing and treatment.

471 In science and technology, increasing the number of researchers in R&D (per million people)
472 significantly increased the DCI. This improvement includes facilitating health science and
473 technology input, strengthening basic life science research, fostering international cooperation
474 between science and technology (such as in the development and use of effective drugs),
475 providing more convenient testing technology, shortening testing times, expanding the scale of
476 detection, improving treatment technology and performing ongoing vaccine development to
477 reduce present and future COVID-19 transmission. In addition, the poverty headcount ratio at the
478 national poverty lines (percentage of population) has a significant negative effect on the IR,
479 CMR and DCI. Increases in the population in poverty and in racial discrimination greatly
480 diminish accessibility to medical services. Government and society must address these problems
481 through economic stimulus plans, unemployment relief programs, welfare and health
482 safeguarding measures, and plans to decrease health spending by these groups [68].

483 We also found that climatic factors (temperature, RH, precipitation and wind speed) did not
484 significantly reduce COVID-19 risk, in agreement with the results of some studies [69].
485 However, previous studies have primarily considered the effects of single climate factors, thus
486 potentially affecting the estimates of the results [70–72]. There is no sufficient evidence
487 indicating that climate factors have specific effects on the spread of COVID-19. This study also
488 shows that in the measurement of COVID-19 risk, the influences of other factors should be
489 considered—such as the constraints of economic development, transportation and other factors—
490 to improve understanding of the mechanisms underlying interrelationships among factors.

491

492 **5. Limitations**

493 This study has several limitations. First, we selected cross-sectional data for spatial analysis and
494 regression modeling; therefore, the results may not reflect more changes in time, thus potentially
495 decreasing the statistical ability to detect the relationships among various factors and COVID-19
496 risk. Second, owing to data matching across databases, some aspects of country/region data may
497 have been lost, thus potentially affecting the spatial weight matrix estimation and regression
498 modeling results. Third, because of the socio-ecological study design, we were unable to access
499 data at the individual level, such as age, sex, occupation, economic and health status, and the
500 actual exposure temperature of each person. However, future studies could adopt hybrid study
501 designs, which use individual-level data from subpopulations to improve ecological
502 extrapolation.

503

504 **6. Conclusion**

505 By using the data from 178 countries/regions, we found that socio-economic factors can
506 significantly reduce the risk of COVID-19. As a next step in COVID-19 prevention, different
507 countries/regions should focus on controlling urban populations, providing economic subsidies
508 and medical resource supplies, and taking broad views of social welfare. Strategies may include
509 population isolation, travel restrictions, case screening, cross-regional or national science and
510 technology exchange to promote diagnosis and treatment, public welfare policy improvement, as
511 well as decreasing the burden of low-income groups in obtaining medical treatment.
512 Simultaneously, we must be alert to the COVID-19 risk in some countries in Africa and Asia,
513 and must curb the second wave of COVID-19 transmission.

514

515 **Acknowledgments**

516 The authors would like to thank the National Natural Science Foundation of China and the
517 National School of Development, Peking University, University of Michigan, and other members
518 for their support and cooperation. We would also like to thank the study samples from The
519 Center for Systems Science and Engineering, Johns Hopkins University (JHU-CSSE), Global
520 Surface Summary of the Day (GSOD) from the Integrated Surface Hourly (ISH) dataset and
521 World Development Indicators (WDI) dataset for providing the information in our research.

522 Contributors: D.S., Y.C.C and X.Y.Z. contributed to the conception and design of the project;
523 D.S., T.Z., K.H., X.Y.Z contributed to the analysis and interpretation of the data; M.T., Y.F.Z.
524 contributed to the data acquisition and provided statistical analysis support; D.S. drafted the
525 article. D.S. and X.Y.Z. are the guarantors. The corresponding author attests that all listed
526 authors meet authorship criteria and that no others meeting the criteria have been omitted.

527

528 **Funding**

529 D.S., Y.C.C., M.T. and Y.F.Z. are funded by National Natural Science Foundation of China (No.
530 71473096; No. 71673101; No. 71974066). X.Y.Z is funded by Michigan Institute for Clinical
531 and Health Research (MICHR No. UL1TR002240).

532

533 **About the Author**

534 Dai Su is a Ph.D. student in the Department of Health Management, School of Medicine and
535 Health Management, Tongji Medical College, Huazhong University of Science and Technology,

536 Wuhan, China. His research interests include infectious diseases, epidemiology, health policy,
537 and health economics.

538

539

540

541 **References**

542 [1] Cleaveland, S., M. K. Laurenson, and L. H. Taylor. "Diseases of humans and their domestic
543 mammals: pathogen characteristics, host range and the risk of emergence." *Philosophical*
544 *Transactions of the Royal Society of London. Series B: Biological Sciences* 356.1411 (2001):
545 991-999.

546 [2] Halliday, Jo EB, et al. "Driving improvements in emerging disease surveillance through
547 locally relevant capacity strengthening." *Science* 357.6347 (2017): 146-148.

548 [3] Schneider, Maria Cristina, and Gustavo Machado. "Environmental and socioeconomic
549 drivers in infectious disease." *The Lancet Planetary Health* 2.5 (2018): e198-e199.

550 [4] Daszak, Peter, Andrew A. Cunningham, and Alex D. Hyatt. "Emerging infectious diseases of
551 wildlife--threats to biodiversity and human health." *science* 287.5452 (2000): 443-449.

552 [5] Weiss, Robin A., and Anthony J. McMichael. "Social and environmental risk factors in the
553 emergence of infectious diseases." *Nature medicine* 10.12 (2004): S70-S76.

554 [6] Woolhouse, Mark EJ, and Sonya Gowtage-Sequeria. "Host range and emerging and
555 reemerging pathogens." *Emerging infectious diseases* 11.12 (2005): 1842.

- 556 [7] Patz, Jonathan A., et al. "Unhealthy landscapes: policy recommendations on land use change
557 and infectious disease emergence." *Environmental health perspectives* 112.10 (2004): 1092-1098.
- 558 [8] Kuhn, K., et al. "Using climate to predict infectious disease outbreaks: A review." *World
559 Health Organization* (2004).
- 560 [9] Wu, XiaoXu, et al. "Impact of global change on transmission of human infectious diseases."
561 *Science China Earth Sciences* 57.2 (2014): 189-203.
- 562 [10] Hamrick, Patricia Najera, et al. "Geographic patterns and environmental factors associated
563 with human yellow fever presence in the Americas." *PLoS neglected tropical diseases* 11.9
564 (2017): e0005897.
- 565 [11] Muñoz-Zanzi, Claudia, et al. "Leptospira contamination in household and environmental
566 water in rural communities in southern Chile." *International journal of environmental research
567 and public health* 11.7 (2014): 6666-6680.
- 568 [12] Semenza, Jan C., et al. "Linking environmental drivers to infectious diseases: the European
569 environment and epidemiology network." *PLoS neglected tropical diseases* 7.7 (2013).
- 570 [13] Froment, A., et al. "Biodiversity and health: the place of parasitic and infectious diseases.
571 Biodiversity change and human health." (2009): 211-227.
- 572 [14] Yang, Hyun M., and Marcelo U. Ferreira. "Assessing the effects of global warming and
573 local social and economic conditions on the malaria transmission." *Revista de saude publica* 34.3
574 (2000): 214-222.
- 575 [15] Martens, Pim, and Susanne C. Moser. "Health impacts of climate change." *Science*
576 292.5519 (2001): 1065-1066.

- 577 [16] McMichael, Anthony J., and Rosalie E. Woodruff. "Detecting the health effects of
578 environmental change: scientific and political challenge." (2005): 1-3.
- 579 [17] Casman, Elizabeth A., and Hadi Dowlatabadi, eds. The contextual determinants of malaria.
580 Resources for the Future, 2002.
- 581 [18] Tol, Richard SJ, and Hadi Dowlatabadi. "Vector-borne diseases, development & climate
582 change." *Integrated Assessment 2.4* (2001): 173-181.
- 583 [19] Epstein, Paul R. "Climate change and emerging infectious diseases." *Microbes and infection*
584 *3.9* (2001): 747-754.
- 585 [20] Wu, Xiaoxu, et al. "Impact of climate change on human infectious diseases: Empirical
586 evidence and human adaptation." *Environment international* *86* (2016): 14-23.
- 587 [21] Wu, XiaoXu, et al. "Impact of global change on transmission of human infectious diseases."
588 *Science China Earth Sciences* *57.2* (2014): 189-203.
- 589 [22] Parham, Paul E., and Edwin Michael. "Outbreak properties of epidemic models: The roles
590 of temporal forcing and stochasticity on pathogen invasion dynamics." *Journal of theoretical*
591 *biology* *271.1* (2011): 1-9.
- 592 [23] Turell, Michael J., Lee W. Cohnstaedt, and William C. Wilson. "Effect of Environmental
593 Temperature on the Ability of *Culex tarsalis* and *Aedes taeniorhynchus* (Diptera: Culicidae) to
594 Transmit Rift Valley Fever Virus." *Vector-Borne and Zoonotic Diseases* (2020).
- 595 [24] Kioutsioukis, Ioannis, and Nikolaos I. Stilianakis. "Assessment of West Nile virus
596 transmission risk from a weather-dependent epidemiological model and a global sensitivity
597 analysis framework." *Acta tropica* *193* (2019): 129-141.

- 598 [25] Peci, Adriana, et al. "Effects of absolute humidity, relative humidity, temperature, and wind
599 speed on influenza activity in Toronto, Ontario, Canada." *Appl. Environ. Microbiol.* 85.6 (2019):
600 e02426-18.
- 601 [26] Sung, Minki, et al. "Airflow as a Possible Transmission Route of Middle East Respiratory
602 Syndrome at an Initial Outbreak Hospital in Korea." *International journal of environmental
603 research and public health* 15.12 (2018): 2757.
- 604 [27] Huang, Chaolin, et al. "Clinical features of patients infected with 2019 novel coronavirus in
605 Wuhan, China." *The Lancet* 395.10223 (2020): 497-506.
- 606 [28] Chen, Nanshan, et al. "Epidemiological and clinical characteristics of 99 cases of 2019
607 novel coronavirus pneumonia in Wuhan, China: a descriptive study." *The Lancet* 395.10223
608 (2020): 507-513.
- 609 [29] Wang, Dawei, et al. "Clinical characteristics of 138 hospitalized patients with 2019 novel
610 coronavirus–infected pneumonia in Wuhan, China." *Jama* (2020).
- 611 [30] Guan, Wei-jie, et al. "Clinical characteristics of coronavirus disease 2019 in China." *New
612 England Journal of Medicine* (2020).
- 613 [31] Liu, Ying, et al. "The reproductive number of COVID-19 is higher compared to SARS
614 coronavirus." *Journal of travel medicine* (2020).
- 615 [32] Parham, Paul E., et al. "Understanding and modelling the impact of climate change on
616 infectious diseases—progress and future challenges." *Climate Change—Socioeconomic Effects*
617 (2011).

- 618 [33] Caldwell, John C. "Rethinking the African AIDS epidemic." *Population and development*
619 *review* 26.1 (2000): 117-135.
- 620 [34] Butler, Colin. "HIV and AIDS, poverty, and causation." *The Lancet* 356.9239 (2000): 1445-
621 1446.
- 622 [35] Auvert, Betran, et al. "Ecological and individual level analysis of risk factors for HIV
623 infection in four urban populations in sub-Saharan Africa with different levels of HIV infection."
624 *Aids* 15 (2001): S15-S30.
- 625 [36] Weiss, Robin A., and Anthony J. McMichael. "Social and environmental risk factors in the
626 emergence of infectious diseases." *Nature medicine* 10.12 (2004): S70-S76.
- 627 [37] Houéto, D. "The social determinants of emerging infectious diseases in Africa." *MOJ Public*
628 *Health* 8.2 (2019): 57-63.
- 629 [38] Wu, Xiaoxu, et al. "Impact of climate change on human infectious diseases: Empirical
630 evidence and human adaptation." *Environment international* 86 (2016): 14-23.
- 631 [39] Kovats, Sari, et al. *Climate change and human health: impact and adaptation*. World Health
632 Organization (WHO), 2000.
- 633 [40] Houéto, D. "The social determinants of emerging infectious diseases in Africa." *MOJ Public*
634 *Health* 8.2 (2019): 57-63.
- 635 [41] Parham, Paul E., et al. "Climate, environmental and socio-economic change: weighing up
636 the balance in vector-borne disease transmission." *Philosophical Transactions of the Royal*
637 *Society B: Biological Sciences* 370.1665 (2015): 20130551.

- 638 [42] Zhang S, Diao M Y, Yu W, et al. Estimation of the reproductive number of Novel
639 Coronavirus (COVID-19) and the probable outbreak size on the Diamond Princess cruise ship: A
640 data-driven analysis[J]. International Journal of Infectious Diseases, 2020, 93: 201-204.
- 641 [43] Li, Qun, et al. "Early transmission dynamics in Wuhan, China, of novel coronavirus–
642 infected pneumonia." New England Journal of Medicine (2020).
- 643 [44] Xie X, Zhong Z, Zhao W, et al. Chest CT for typical 2019-nCoV pneumonia: relationship to
644 negative RT-PCR testing[J]. Radiology, 2020: 200343.
- 645 [45] Dong, Ensheng, Hongru Du, and Lauren Gardner. "An interactive web-based dashboard to
646 track COVID-19 in real time." The Lancet Infectious Diseases (2020).
- 647 [46] Chen, Biqing, et al. "Roles of meteorological conditions in COVID-19 transmission on a
648 worldwide scale." medRxiv (2020).
- 649 [47] Anselin, Luc. "A local indicator of multivariate spatial association: extending Geary's C."
650 Geographical Analysis 51.2 (2019): 133-150.
- 651 [48] Elhorst, J. Paul, Donald J. Lacombe, and Gianfranco Piras. "On model specification and
652 parameter space definitions in higher order spatial econometric models." Regional Science and
653 Urban Economics 42.1-2 (2012): 211-220.
- 654 [49] Phung, Dung, et al. "The effects of socioecological factors on variation of communicable
655 diseases: A multiple-disease study at the national scale of Vietnam." PloS one 13.3 (2018).
- 656 [50] Hondula, David M., and Adrian G. Barnett. "Heat-related morbidity in Brisbane, Australia:
657 spatial variation and area-level predictors." Environmental health perspectives 122.8 (2014):
658 831-836.

- 659 [51] Armocida, Benedetta, et al. "The Italian health system and the COVID-19 challenge." The
660 Lancet Public Health (2020).
- 661 [52] Leung, Kathy, et al. "First-wave COVID-19 transmissibility and severity in China outside
662 Hubei after control measures, and second-wave scenario planning: a modelling impact
663 assessment." The Lancet (2020).
- 664 [53] Kraemer, Moritz UG, et al. "The effect of human mobility and control measures on the
665 COVID-19 epidemic in China." Science (2020).
- 666 [54] Chinazzi, Matteo, et al. "The effect of travel restrictions on the spread of the 2019 novel
667 coronavirus (COVID-19) outbreak." Science (2020).
- 668 [55] Prem, Kiesha, et al. "The effect of control strategies to reduce social mixing on outcomes of
669 the COVID-19 epidemic in Wuhan, China: a modelling study." The Lancet Public Health (2020).
- 670 [56] Koo, Joel R., et al. "Interventions to mitigate early spread of SARS-CoV-2 in Singapore: a
671 modelling study." The Lancet Infectious Diseases (2020).
- 672 [57] Xu, Shunqing, and Yuanyuan Li. "Beware of the second wave of COVID-19." The Lancet
673 (2020).
- 674 [58] Niehus, Rene, et al. "Using observational data to quantify bias of traveller-derived COVID-
675 19 prevalence estimates in Wuhan, China." The Lancet Infectious Diseases (2020).
- 676 [59] Martinez-Alvarez, Melisa, et al. "COVID-19 pandemic in west Africa." The Lancet Global
677 Health (2020).
- 678 [60] Lee, Vernon J., et al. "Epidemic preparedness in urban settings: new challenges and
679 opportunities." The Lancet Infectious Diseases (2020).

- 680 [61] Dowd, Jennifer Beam, et al. "Demographic science aids in understanding the spread and
681 fatality rates of COVID-19." medRxiv (2020).
- 682 [62] Sajadi, Mohammad M. and Habibzadeh, Parham and Vintzileos, Augustin and Shokouhi,
683 Shervin and Miralles-Wilhelm, Fernando and Amoroso, Anthony, Temperature, Humidity and
684 Latitude Analysis to Predict Potential Spread and Seasonality for COVID-19 (March 5, 2020).
685 Available at SSRN: <https://ssrn.com/abstract=3550308> or <http://dx.doi.org/10.2139/ssrn.3550308>
- 686 [63] Ruan, Shigui. "Likelihood of survival of coronavirus disease 2019." *The Lancet Infectious
687 Diseases* (2020).
- 688 [64] Fang, Lei, George Karakiulakis, and Michael Roth. "Are patients with hypertension and
689 diabetes mellitus at increased risk for COVID-19 infection?." *The Lancet. Respiratory Medicine*
690 (2020).
- 691 [65] Ayebare, Rodgers R., et al. "Adoption of COVID-19 triage strategies for low-income
692 settings." *The Lancet Respiratory Medicine* (2020).
- 693 [66] Chen, Simiao, et al. "Fangcang shelter hospitals: a novel concept for responding to public
694 health emergencies." *The Lancet* (2020).
- 695 [67] Miani, Alessandro, et al. "The Italian war-like measures to fight coronavirus spreading: Re-
696 open closed hospitals now." *EClinicalMedicine* (2020).
- 697 [68] McCloskey, Brian, et al. "Mass gathering events and reducing further global spread of
698 COVID-19: a political and public health dilemma." *Lancet* (London, England) 395.10230 (2020):
699 1096.

- 700 [69] Yao, Y., Pan, J., Liu, Z., Meng, X., Wang, W., Kan, H., & Wang, W. (2020). No
701 Association of COVID-19 transmission with temperature or UV radiation in Chinese cities. The
702 European respiratory journal, 2000517. Advance online publication.
703 <https://doi.org/10.1183/13993003.00517-2020>
- 704 [70] Islam, Nazrul, Sharmin Shabnam, and A. Mesut Erzurumluoglu. "Meteorological factors
705 and Covid-19 incidence in 310 regions across the world." medRxiv (2020).
- 706 [71] Zhu, Yongjian, and Jingui Xie. "Association between ambient temperature and COVID-19
707 infection in 122 cities from China." Science of The Total Environment (2020): 138201.
- 708 [72] Wang, Mao, et al. "Temperature significant change COVID-19 Transmission in 429 cities."
709 medRxiv (2020).